NeuroImage: Clinical 12 (2016) 219–226

Contents lists available at ScienceDirect

NeuroImage: Clinical

journal homepage: www.elsevier.com/locate/ynicl

Diffusivity in multiple sclerosis lesions: At the cutting edge?☆

Alexander Klistorner[a,b,*], Chenyu Wang[c], Vera Fofanova[b], Michael H. Barnett[c], Con Yiannikas[d], John Parratt[d], Yuyi You[a,b], Stuart L. Graham[b]

[a]Save Sight Institute, Sydney Medical School, University of Sydney, Sydney, Australia
[b]Faculty of Medicine and Health Sciences, Macquarie University, Sydney, NSW, Australia
[c]Brain and Mind Research Institute, Sydney Medical School, University of Sydney, Sydney, NSW, Australia
[d]Royal North Shore Hospital, Sydney, NSW, Australia

ARTICLE INFO

Article history:
Received 20 April 2016
Received in revised form 4 June 2016
Accepted 4 July 2016
Available online 05 July 2016

ABSTRACT

Background: Radial Diffusivity (RD) has been suggested as a promising biomarker associated with the level of myelination in MS lesions. However, the level of RD within the lesion is affected not only by loss of myelin sheaths, but also by the degree of tissue destruction. This may lead to exaggeration of diffusivity measures, potentially masking the effect of remyelination.
Objective: To test the hypothesis that the T2 hyperintense lesion edge that extends beyond the T1 hypointense lesion core is less affected by tissue loss, and therefore a more appropriate target for imaging biomarker development targeting de- and re-myelination.
Method: Pre- and post-gadolinium (Gd) enhanced T1, T2 and DTI images were acquired from 75 consecutive RRMS patients. The optic radiation (OR) was identified in individual patients using a template-based method. T2 lesions were segmented into T1-hypointense and T1-isointense areas and lesion masks intersected with the OR. Average Radial, Axial and Mean diffusivity (RD, AD and MD) and fractional anisotropy (FA) were calculated for lesions of the entire brain and the OR. In addition, Gd enhancing lesions were excluded from the analysis.
Results: 86% of chronic T2 lesions demonstrated hypointense areas on T1-weighted images, which typically occupied the central part of each T2 lesion, taking about 40% of lesional volume. The T1-isointense component of the T2 lesion was most commonly seen as a peripheral ring of relatively constant thickness ("T2-rim"). While changes of diffusivity between adjacent normal appearing white matter and the "T2-rim" demonstrated a disproportionally high elevation of RD compare to AD, the increase of water diffusion was largely isointense between the "T2-rim" and T1-hypointense parts of the lesion.
Conclusion: Distinct patterns of diffusivity within the central and peripheral components of MS lesions suggest that axonal loss dominates in the T1 hypointense core. The effects of de/remyelination may be more readily detected in the "T2-rim", where there is relative preservation of structural integrity. Identifying and separating those patterns has an important implication for clinical trials of both neuroprotective and, in particular, remyelinating agents.

1. Introduction

Recent interest in the development of remyelinating therapies has increased demand for reliable in vivo surrogate markers of remyelination. Quantification of the diffusion characteristics of brain tissue, in particular Radial Diffusivity, has been suggested as a promising imaging biomarker associated with the level of tissue myelination. Experimental models of demyelination have demonstrated a close correlation between degree of myelin loss and alterations in RD (Song et al., 2005; Janve et al., 2013). In post-mortem studies of human MS brains, elevation of RD was topographically linked to areas of histologically identified demyelination (Schmierer et al., 2007; Schmierer et al., 2008; Wang et al., 2015). A close relationship between increase in RD and electrophysiological measures of demyelination was also reported in patients with MS (Alshowaeir et al., 2014). However, some recent studies have failed to demonstrate an unequivocal relationship between increased RD and the degree of demyelination, suggesting that this measure is not pathologically specific (Klawiter et al., 2012).

Currently, conventional MRI is the gold standard to identify focal inflammatory demyelination in MS. Typically, acute T2 lesions comprise an area of demyelination and surrounding edema. Resolution of acute inflammation and edema are probably responsible for reduction in lesion size, with a permanent residual lesion that includes demyelinated

☆ Supported by grant from National Multiple Sclerosis Society (NMSS), Novartis Save Neuron Grant, Sydney Eye Hospital foundation grant YY is National Health and Medical Research Council (NHMRC) fellow.
* Corresponding author at: Save Sight Institute, University of Sydney, 8 Macquarie St. Sydney, NSW 2000, Australia.
E-mail address: sasha.klistorner@sydney.edu.au (A. Klistorner).

http://dx.doi.org/10.1016/j.nicl.2016.07.003

(and partially remyelinated) axons (Schmierer et al., 2009) and areas of expanded extracellular space. The widening of extracellular space is believed to be caused by tissue destruction and may occupy up to 87% of the lesion volume (Barnes et al., 1991; Miller, 2008). The majority of chronic T2 lesions are also seen as hypointense areas on T1-weighted images, although typically the change of the signal intensity on the T1-weighted image occurs only in part of the T2 lesion (Barkhof and van Walderveen, 1999). The level of T1 hypointensity varies significantly from slightly hypointense in comparison to surrounding NAWM to approaching the intensity of CSF, reflecting a variable degree of widening of the extracellular space (Loevner et al., 1995; Van Waesberghe et al., 1998; Miller, 2008).

The extent of lesional tissue loss is also closely linked to DTI measures, since expansion of extra-cellular space dramatically increases isotropic diffusion of water molecules (Rovaris et al., 2005). Therefore, it is highly likely that the level of RD within the lesion is affected not only by loss of myelin sheath, but also by the level of tissue destruction. Tissue destruction may therefore 'exaggerate' both RD and AD (Wang et al., 2011), masking the potential effect of remyelination on diffusivity measures.

The purpose of this study was to examine diffusivity indices in T2 and T1 lesions of MS patients. Since T1 changes, which are closely relate to loss of tissue matrix, constitute only part of a T2 lesion, we hypothesized that the T2 hyperintense lesion edge that extends beyond the T1 hypointense lesion core (which we called "T2-rim" area) may be less affected by tissue loss, and therefore be a better target for studying the effects of de/remyelination.

The specificity of altered diffusion for pathologic changes is limited by the wide spectrum of normal anisotropy indices in the brain (Bammer et al., 2000). We studied lesions in the optic radiations, highly organized fibre tracts that are a frequent site of MS pathology, to facilitate accurate measurement of relative diffusivity change along axonal bundles (Mädler et al., 2008). In addition, internal structure of the OR does not contain a significant number of crossing fibers, which can potentially (and sometimes paradoxically) alter diffusivity (Yeatman et al., 2012; Winston, 2012). This point is especially pertinent considering the issues that surround misalignment between corresponding eigenvectors with the underlying tissue structures (Wheeler-Kingshott and Cercignani, 2009).

2. Material and methods

The study was approved by University of Sydney and Macquarie University Human Research Ethics Committees. All procedures followed the tenets of the Declaration of Helsinki and written informed consent was obtained from all participants.

2.1. Subjects

Seventy-five consecutive patients with Relapsing-Remitting MS (RRMS) and no history of clinical optic neuritis (ON) in at least one eye were enrolled. RRMS was defined according to standard criteria (Polman et al., 2011). A history of ON was based on the patient's clinical notes and the absence of previous symptoms. Patients with any other systemic or ocular disease, in particular those that could potentially affect our measurement parameters were excluded.

2.2. MRI protocol

The following sequences were acquired using a 3T GE Discovery MR750 scanner (GE Medical Systems, Milwaukee, WI):

1. Pre- and postcontrast (gadolinium) Sagittal 3D T1: GE BRAVO sequence, FOV 256 mm, Slice thickness 1 mm, TE 2.7 ms, TR 7.2 ms, Flip angle 12°, Pixel spacing 1 mm. Acquisition Matrix (Freq. × Phase) is 256 × 256, which results in 1 mm isotropic acquisition voxel size. The reconstruction matrix is 256 × 256.

2. FLAIR CUBE; GE CUBE T2 FLAIR sequence, FOV 240 mm, Slice thickness 1.2 mm, Acquisition Matrix (Freq. × Phase) 256 × 244, TE 163 ms, TR 8000 ms, Flip angle 90°, Pixel spacing 0.47 mm. The reconstruction matrix is 512 × 512.

3. Whole brain 64-directions diffusion weighted imaging with 2 mm isotropic acquisition matrix (TR/TE = 8325/86 ms, b = 1000 s/mm^2, number of b0s = 2).

2.3. Reconstruction of individual optic radiations

Individual optic radiation masks was reconstructed from in-house optic radiation template through non-linear registration as follow:

1. 3DT1 images were lesion-inpainted (FSL) using T2 lesion masks,
2. individual brain masks were derived using Brain Extraction Tool from FSL with manual quality control,
3. deformation maps were obtained from non-linear registration between individual brain and ICBM 2009a standard brain template (Fonov et al., 2011),
4. in-house optic radiation template was mapped into individual patient's space through the deformation map.

2.4. Lesion identification and analysis

Whole brain T2 lesions were identified on the co-registered T2 FLAIR images and segmented semi-automatically using ITK-SNAP 3 software (http://www.itksnap.org) by a trained analyst. To minimize partial volume effect, only T2 lesions with a volume larger than 100 mm^3 were evaluated.

T1 lesions were identified on pre-contrast 3D-T1-weighted images. They were defined as regions with low signal intensity relative to the surrounding white matter and corresponded with an area of high signal intensity on T2. The lesion (hypo-) intensity was not quantified. T2 lesions demonstrating Gd-enhancement were excluded from analysis. Similar to T2 lesions, T1 lesions were segmented semi-automatically using ITK-SNAP 3 software by a trained analyst (VF). Both T2 and T1 lesion segmentation was verified by two more persons, who have extensive experience in lesion segmentation (AK, CW). Occasional discrepancies were resolved by consensus.

Each T1 hypointense lesion typically occupied the central area of a T2 lesion, leaving the peripheral part of the T2 lesion T1-isointense. We called this part of the T2 lesion the "T2-rim" (Fig. 1). A minority of T2 lesions did not display T1 hypointensity; these lesions were typically small or had a linear, elongated shape (blue arrowheads in Fig. 1), contributing little to the total T2 lesion volume. Therefore, for the purpose of analysis, T1-hypointense and T2-rim areas of T2 lesions were evaluated separately.

Since the majority of lesions had a spherical shape, we calculated radius of T2 and T1 lesions by dividing the total lesion load by the lesion number. In addition, the width of the T2-rim area was calculated as a difference between the radii of T2 and T1 lesions.

Lesion masks were then intersected with the OR to identify and measure the volume of T2, T1 and T2-rim lesions within the OR, as described in detail elsewhere (Klistorner et al., 2015).

For single lesion analysis, only well demarcated T2 lesions with no visible abnormality in the corresponding part of contralateral OR on both T2 and T1 images were selected. The region of the contralateral OR corresponding in volume and position to T2 lesion was used as a reference representing NAWM (Fig. 2).

3. Results

Seventy-five consecutive RRMS patients (age: 41.6 ± 10.1, disease duration: 4.9 ± 3.6 years, 25M/50F, EDSS score: 1.42 ± 1.38) were enrolled in the study. Patients with any other systemic or ocular diseases were excluded. All patients were relapse-free for at least 3 months

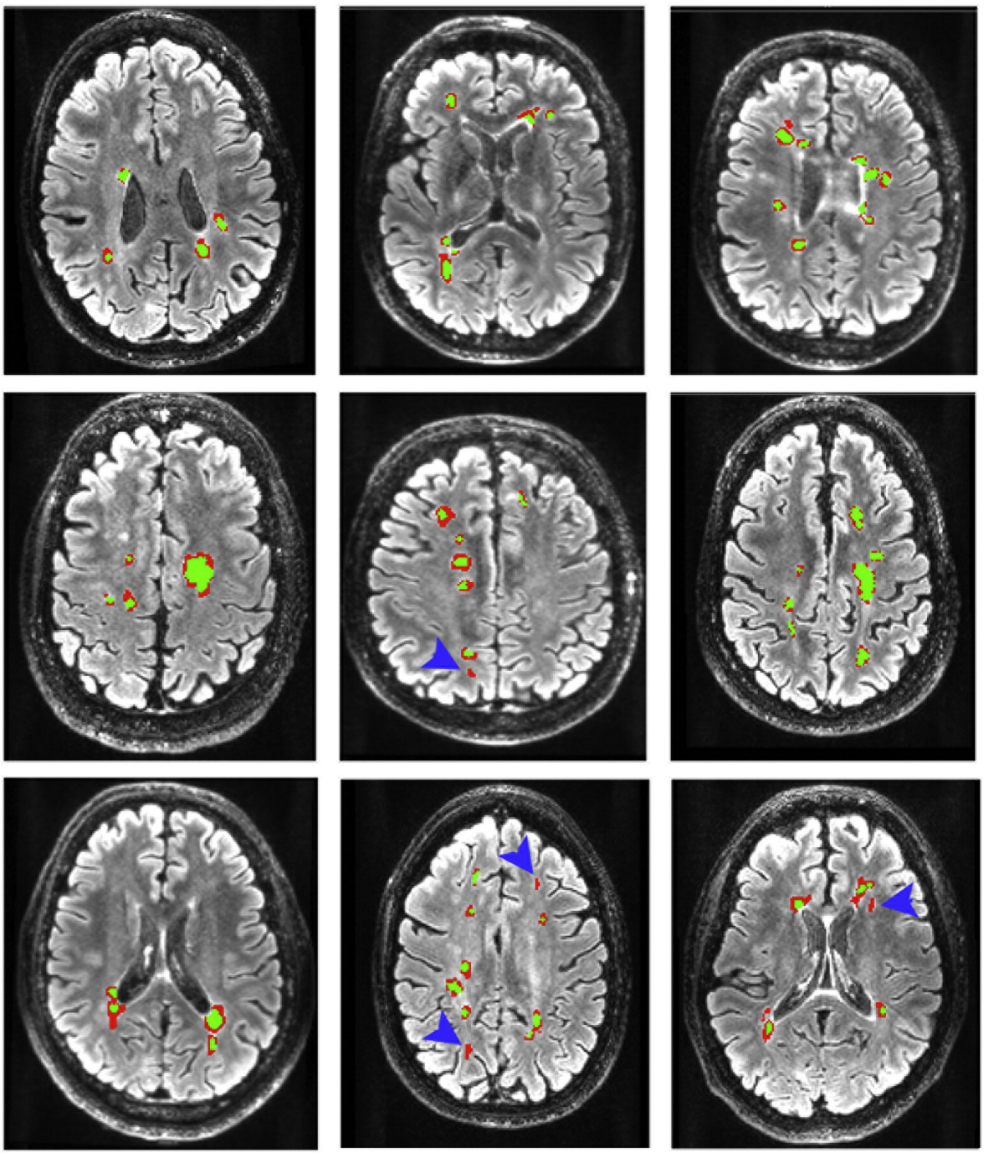

Fig. 1. Examples of lesion segmentation. Green-T1 hypointense area, Red-"T2-rim" area. Blue arrowheads denote T2 lesions without corresponding T1 hypointensity. (For interpretation of the references to color in this figure legend, the reader is referred to the web version of this article.)

prior to the enrolment. Seventy patients (93%) were receiving disease-modifying therapy at the time of enrolment (7-Betaferon, 20-Copaxon, 25-Gylenia, 6-Tysabril, 8-Avonex, 2-Tecfidera, 2-Rebif).

A history of optic neuritis (ON) in one eye was not an exclusion criteria, however, none of the patients had ON or visual disturbances within 6 months of baseline assessment. **All patients with history of ON received steroid as part of ON treatment.**

There were total of 849 lesions identified on T2-FLAIR scans (Table 1). Of these, 726 lesions (86%) demonstrated (partial) hypointensity on T1 images. The mean T1 lesion volume constituted approximately 41% of T2 lesion volume. There was highly significant correlation between T2 and T1 lesion number, lesion volume and average single lesion radius ($r^2 = 0.96$, 0.92 and 0.86 respectively, $p < 0.001$ for all) (Fig. 3 below). However, while the volume of the T2-rim area correlated

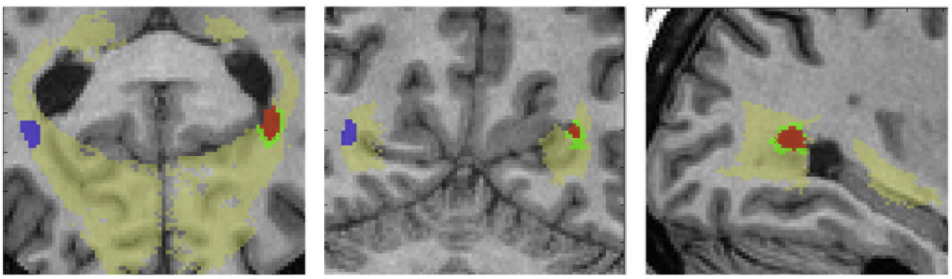

Fig. 2. Analysis of single optic radiation lesion.

Table 1
Whole brain lesions (Mean ± SD).

	Number of lesions	Lesion volume mm^3	Average volume of single lesion, mm^3	Average radius of single lesion, mm
T2 lesions	849	5546 ± 6001	430 ± 211	4.64 ± 0.75
T1 lesions	726	2191 ± 2798	187 ± 119	3.45 ± 0.74
T2-rim area	849	3852 ± 3544	267 ± 119	1.2 ± 0.29 (width)

significantly with total T2 lesion volume ($r^2 = 0.95$, $p < 0.001$), there was no correlation between width of T2-rim ring and T2 lesion radius ($r^2 = 0.049$, $p > 0.05$) indicating that the width of the T2-rim is independent of the volume of T2 lesion, and remains relatively constant.

Of 75 patients, 63 (84%) demonstrated T2 lesions within the ORs. The mean volume of OR T2, T1 and T2-rim area was 1303 ± 1269, 460 ± 558 and 836 ± 771 mm^3 respectively. There was a highly significant correlation between OR T2 and T1 lesion volumes ($R^2 = 0.88$) (Fig. 4). OR lesion volume also correlated significantly with whole brain lesion volume ($r^2 = 0.74$ and $r^2 = 0.70$ for T2 and T1 lesions respectively).

3.1. DTI analysis

Diffusivity coefficients of entire OR and OR lesions (total T2 lesions, T1 and T2-rim areas) are presented in Table 2.

Both RD and AD of the OR demonstrated highly positive correlations with OR T2 lesion load ($r^2 = 0.69$ and $r^2 = 0.46$ respectively, $p < 0.001$ for both) and OR T1 lesion load ($r^2 = 0.59$ and $r^2 = 0.48$ respectively, $p < 0.001$ for both), while OR FA was negatively correlated with volume of OR lesions ($r^2 = -0.53$ and $r^2 = -0.40$ for T2 and T1 lesions respectively, $p < 0.001$ for both) (Fig. 5).

Compartmentalization of T2 lesions revealed that both AD and RD were significantly higher in T1 areas compared to the T2-rim area, producing a 21% rise in MD value between the two. While absolute change in diffusivity between T2-rim and T1 areas was very similar for both RD and AD (0.20 and 0.24), RD demonstrated slightly larger relative increase compare to AD (24% vs 17% for RD and AD respectively), which resulted in a small, but significant drop of FA between T2-rim and T1 areas (−0.03 or 8.8%). In addition, AD and RD were highly correlated between each other in T1 lesional areas ($r^2 = 0.63$, $p < 0.001$), suggesting predominantly isotropic diffusivity, while in T2-rim areas the correlation was less apparent ($r^2 = 0.31$, $p < 0.01$) (Fig. 6).

We have recently reported a very different pattern of diffusivity change between OR lesional (T2) tissue and OR NAWM in a similar cohort of MS patients (Klistorner et al., 2015), which demonstrated more significant increase of RD compare to AD, resulting in substantial drop of FA (18%) (Fig. 7). Since in the previous study the entire T2 lesional area (including the T1 component) was analysed, it is reasonable to assume that the difference between increase of RD and AD at the NAWM/T2-rim border (and, as a result, the drop in FA) is even higher.

To confirm this we performed the analysis of diffusivity in individual OR lesions. Twenty-seven subjects had isolated T2 lesions on one side of the OR and normal looking white matter in the corresponding part of the contralateral OR (which was used as a reference area analogous to NAWM). Diffusivity of T1 and T2-rim areas of the lesions were measured separately.

The result of this single lesion analysis (Table 3) demonstrated that RD continued to increase from NAWM to T2-rim area and then to T1 area with equal increments (0.20 and 0.20) The gradient of AD rise, however, increased from 0.10 at the border between NAWM and T2-rim area to 0.20 at the border between T2-rim and T1 areas. This was reflected in a more substantial drop of FA at NAWM/T2-rim border (−0.12) compared to T2-rim/T1 border (−0.05).

In addition, a significant positive correlation was found between the level of diffusivity in T2 lesions and the proportion of the lesion occupied by T1 hypointensity (Fig. 8). Linear Regression analysis indicated that not only >65% of AD variability, but also more than half of RD variability in T2 lesions can be explained by the relative size of T1 hypointensity and, therefore, is related to the extent (and probably severity) of axonal loss.

4. Discussion

In the current study we examined the directional diffusivity in OR lesions of RRMS patients. Application of novel compartmentalized approach suggested new way of assessing lesional diffusivity which may facilitate the measurement of demyelination/remyelination in deep brain lesions and potentially serve as an outcome measure in therapeutic trials of emerging pro-reparative treatment.

We demonstrated a high correlation of both T2 and T1 OR lesion volume with whole brain lesional load, supporting the use of the OR as a model of pathological activity in MS. We also confirmed our previous observation that the major part of OR DTI variability is associated with lesional damage (Klistorner et al., 2014). However, while RD is more dependent on lesion volume, the variation of AD is probably impacted by other factors, including severity of the structural damage within the lesions and Wallerian degeneration (Klistorner et al., 2015).

Various patterns of abnormal diffusivity in T2 vs T1 lesions have been previously described in MS. In chronic lesions the most common finding was increased water diffusion (ADC or MD) and reduced FA in lesional tissue compared to NAWM; and more marked diffusion alterations were present in T1 hypointense lesions compared to T1 isointense lesions (Filippi et al., 2001; Droogan et al., 1999; Bammer et

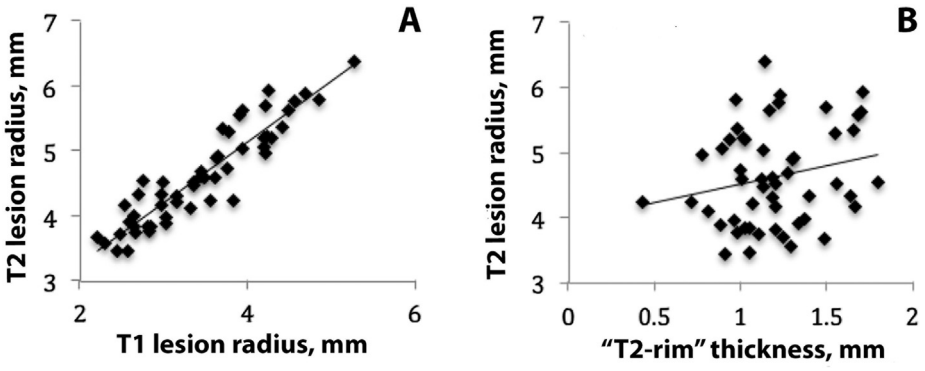

Fig. 3. Correlation between T2 lesion radius and: a) T1 lesion radius, b) T2-rim area width.

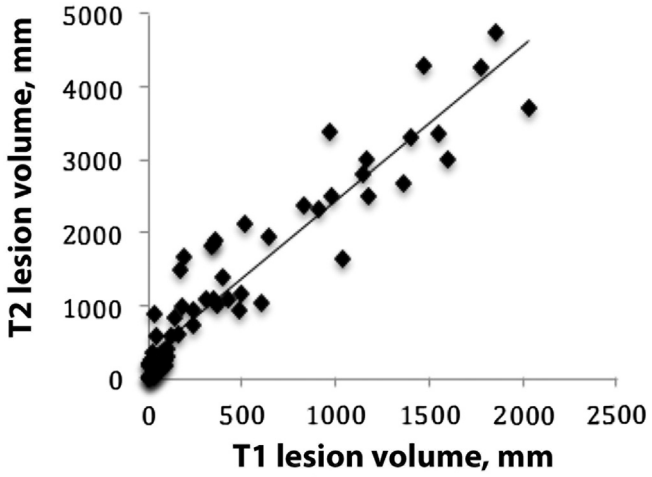

Fig. 4. Correlation between OR T2 and T1 lesion volume.

al., 2000; Scanderbeg et al., 2000; Werring et al., 1999; or see Sbardella et al., (2013) for review).

Since primary identification of the lesions was always based on T2-weighted (and proton density) images, in earlier studies the term "T1 isointense lesion" simply meant "pure" (i.e. not detectable on T1 images) T2 lesions, while the term "T1 hypointense lesion" was used to mark those T2 lesions which contained areas of low signal intensity on T1 non-contrast images. The relative number of reported hypointense T1 lesions varied between studies from as low 10% to as high as 70% of total lesion number (Filippi et al., 2001; Werring et al., 1999; Bammer et al., 2000; Nusbaum et al., 2000). This disagreement can potentially be related to the different definitions of T1 hypointensity. Thus, in some studies the intensity of the lesions on T1 images was compared to the surrounding NAWM (Filippi et al., 2001; Scanderbeg et al., 2000; Werring et al., 1999), while in others-to the grey matter (Nusbaum et al., 2000), while in others several levels of hypointensity were used(Loevner et al., 1995).

Here we used the most frequently reported definition of T1 hypointensity: an area of low T1 signal intensity in comparison to the surrounding NAWM. We demonstrated that the vast majority (86%) of T2 lesions correspond with areas of T1 hypointensity. The high rate of detection of the T1 hypointensity found in our study may partially be explained by the better resolution of our imaging technique, which employed 1 mm slices, compared to 5 mm slice thickness used in earlier studies and use of 3D T1 sequence. In addition, inclusion of slightly hypointense lesions may also increase the rate of T1 lesions reported here.

Segmentation of the T2 lesions was also performed differently from some of the earlier studies. Previously the entire area of T2 lesions displaying abnormal T1 signal was marked and analysed as "T1 hypointense lesion", even if it was only partially occupied by T1 hypointensity (as was frequently the case) (Loevner et al., 1995; Filippi et al., 2001; Bammer et al., 2000; Werring et al., 1999). In the current study, however, every lesion displaying T1 signal abnormality was segmented (compartmentalized) into two areas: genuine T1 area (which represented a part of T2 lesion seen as hypointense area on T1-weighted images) and "T2-rim" area, which corresponded with the component of the T2 lesion not visible (i.e. isointense) on T1-weighted images. Diffusivity of both areas was analysed separately, an approach that we hypothesized would provide better insight into the nature of diffusivity and its relationship with demyelinating and destructive components of lesional pathology.

Table 2
Diffusivity coefficients of OR and OR lesions (Mean (SD)).

	AD	RD	FA	MD
Entire OR	1.17 (0.04)	0.68 (0.05)	0.35 (0.03)	0.85 (0.05)
T2 lesions	1.47 (0.15)	0.87 (0.10)	0.33 (0.04)	1.07 (0.11)
T1 area	1.62 (0.22)	1.00 (0.14)	0.31 (0.05)	1.22 (0.14)
T2-rim area	1.39 (0.17)	0.81 (0.08)	0.34 (0.05)	1.01 (0.08)

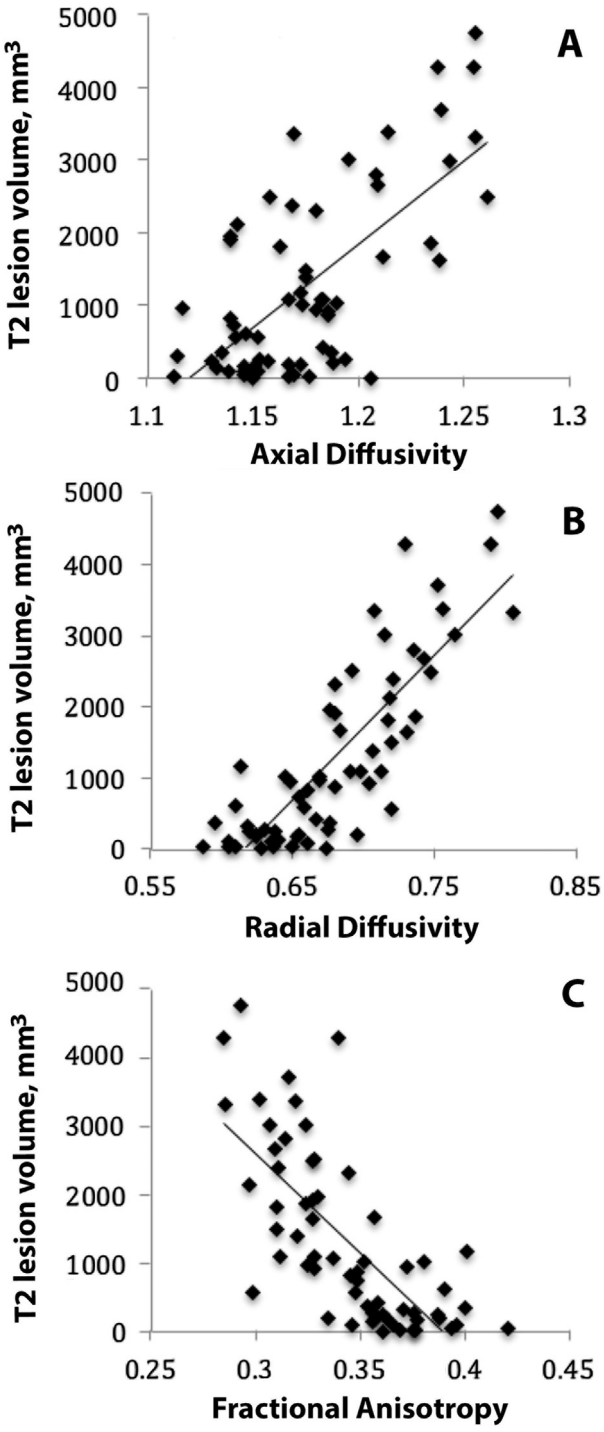

Fig. 5. Correlation between OR T2 lesion volume and OR diffusivity coefficients including AD, RD and FA.

In addition, the use of primary eigenvalues (AD and RD) rather than composite indices (ADC, MD or FA) employed in earlier studies, may also be beneficial in understanding mechanisms of diffusivity change(Aung et al., 2014; Klistorner et al., 2015; Schmierer et al., 2007).

Segmentation of T2 lesions demonstrated that the area of T1 hypointensity typically occupies the central area of the lesion, leaving

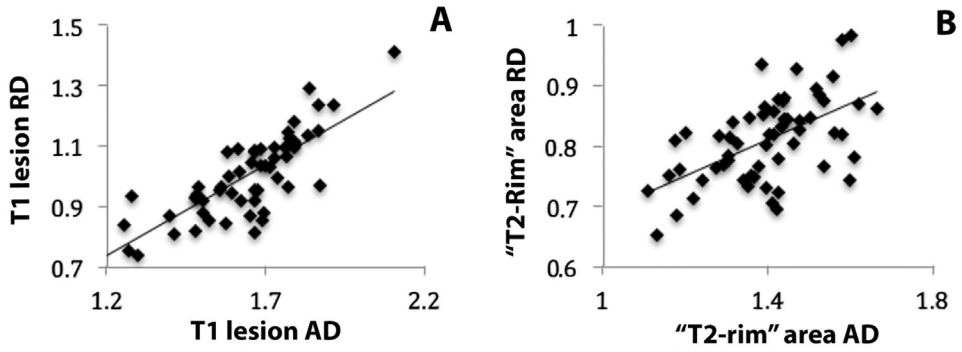

Fig. 6. Correlation between AD and RD in: a) T1 area, b) "T2-rim" area.

the periphery of the lesion T1-isointense, presumably reflecting distinct pathological changes occurring within the lesion. T2-hyperintensity, while pathologically non-specific, marks the external border of the entire chronically demyelinated area (Schmierer et al., 2009). Conversely, T1 hypointensity is linked to more severe tissue damage caused by axonal loss and resulting widening of the extracellular space (Loevner et al., 1995; Van Waesberghe et al., 1998; van Walderveen et al., 1998; Brex et al., 2000). Therefore, destructive changes are likely to primarily impact MRI appearance and diffusion metrics in the central part of the lesion, masking to a large degree any effect of demyelination. In contrast, relative preservation of axons in the peripheral part of the lesion would render demyelination the key pathological feature. As a consequence, the rim of the lesion, while isointense on T1, remains visible on T2-weighted images.

This hypothesis is supported by OR diffusivity data. While the current study revealed a significant increase of diffusivity (both RD and AD) toward the center of the lesion, RD demonstrated a disproportionally high (in relation to AD) increase between NAWM and T2-rim areas in comparison with the changes observed between T2-rim and T1 areas. This resulted in a reduced rate of FA decline, which changed from 0.12 at the NAWM/T2-rim border to only 0.05 at T2-rim/T1 border.

Since an increase of RD (but not AD) is believed to be related to the degree of demyelination (Schmierer et al., 2007; Klawiter et al., 2011; Song et al., 2005), our results, which show a much larger change of RD compared to AD at the NAWM/T2-rim border, suggest significant loss of myelin in T2-rim area. In contrast, similar changes of RD and AD at T2-rim/T1 border imply more isotropic diffusion in the central (T1) part of the lesion, which is indicative of severe tissue destruction and widening of the extracellular space, in agreement with the previously reported association between lesion T1 hypointensity and the degree of diffusion (Scanderbeg et al., 2000; Werring et al., 1999; Filippi et al., 2000; Rovaris et al., 2005). Differences in directional diffusivity between T2-rim and T1 areas are also reflected in a larger reduction of FA at NAWM/T2-rim compare to T2-rim/T1 borders.

The mostly isotropic diffusion in T1 lesions also reflects a very high correlation between AD and RD within this area, while in T2-rim areas the correlation was less apparent ($r^2 = 0.63$ vs 0.31). This also supports the assumption that a mechanism responsible for the comparable increase of both RD and AD (such as enlargement of an extra-cellular space due to axonal loss) dominates the changes in diffusivity in the T1 area.

Compared to T1 lesions the standard deviation of RD in T2-rim areas was notably smaller, possibly reflecting similar degree of demyelination, whereas the severity of tissue destruction and axonal loss, which is an additional factor contributing to the magnitude of diffusivity in the T1 area, may vary considerably (Kolasinski et al., 2012; van Walderveen et al., 1998; Lassmann et al., 1994).

An alternative explanation for the different patterns of diffusivity in the peripheral vs central part of the lesion could be partial remyelination, which is typically observed at the border of the chronic MS lesion and is likely to be visible on T2-weighted images as a mildly hyperintense area (Nijeholt et al., 2001)(van Walderveen et al., 1998). It is conceivable that more severe loss of myelin in the central area of the lesion contributes to widening of the extracellular space (particularly considering the large relative volume of myelin sheath compare to axonal volume (Mohammadi et al., 2015)). However, based on the notion that an increase in RD is linked to loss of myelin, while change of AD is largely associated with axonal degeneration, severe demyelination alone could not explain the mostly isotropic nature of diffusivity increase toward the center of the lesion.

Regardless of the origin of the expanded extra-cellular space (which may be a combined effect of axonal loss, severe demyelination and post-inflammatory cavitation), increased tissue water content alone will result in an isotropic rise in diffusivity, reducing the potential sensitivity of RD to de/remyelination (Klawiter et al., 2011; Wang et al., 2015; Wang et al., 2011). This is consistent with our finding that isotropic

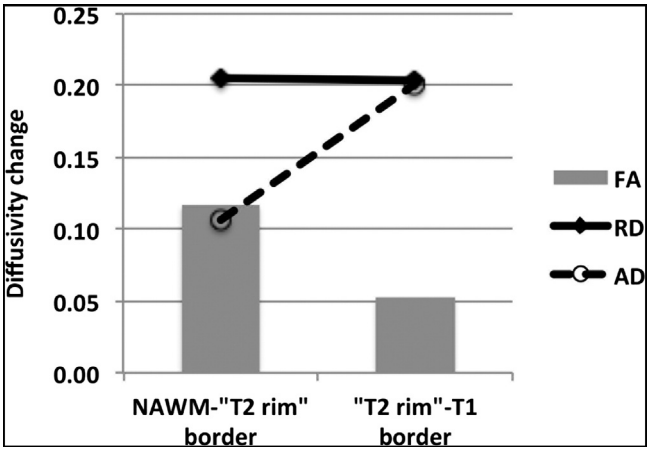

Fig. 7. Change of diffusivity coefficients at the borders of NAWM-"T2-rim" area and "T2-rim"-T1 area. While RD increases to exactly the same amount between NAWM and "T2-rim" area and between "T2-rim" area and T1 area, increase of AD is much more pronounced between "T2-rim" area and T1 area compare to border between NAWM and "T2-rim" area. This results in significantly larger drop of FA between NAWM and "T2-rim" area compare to border between "T2-rim" area and T1 area. Vertical axis represents change in diffusivity for RD, AD (μm^2/ms for both) and FA (arbitrary units).

Table 3
Diffusivity coefficients of OR single lesions (Mean (SD)).

	AD	RD	FA	MD
NAWM	1.39 (0.11)	0.61 (0.07)	0.49 (0.05)	0.87 (0.06)
T2-rim area	1.49 (0.12)	0.82 (0.08)	0.37 (0.05)	1.04 (0.07)
T1 area	1.69 (0.15)	1.02 (0.17)	0.32(0.07)	1.25 (0.15)

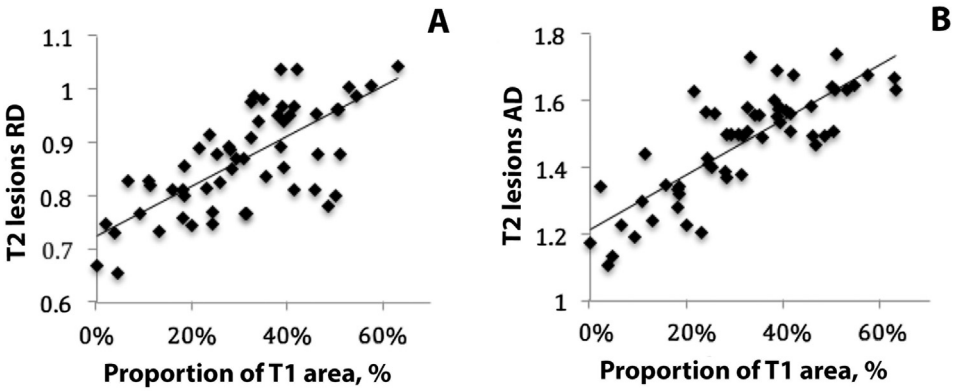

Fig. 8. Correlation between lesional diffusivity and proportional size of the T1 hipointense area within T2 lesion: a) RD, b) AD.

increase of diffusivity in the T1 lesion area significantly contributes to RD of the T2 lesion area.

Another important observation in the current study relates to the width of T2-rim area, which remained constant regardless of the lesion volume. While the significance of this fact remains obscure, it may reflect relative preservation of axons at the lesion edge. Conversely, it may be related to the partial remyelination, which is often limited to the lesion border. We previously demonstrated that the degree of remyelination following optic neuritis, is relatively constant and does not correlate with lesion size (Klistorner et al., 2010). However, since axonal survival and remyelination are intimately linked (preserved axons are needed to initiate remyelination, while remyelinated fibers are better preserved), a combination of both factors may be responsible for the phenomenon observed in this study. The constant T2-rim width may also explain why small T2 lesions with a linear, elongated shape do not always display associated T1 hypointensity; T2-rim areas from opposite sides of the lesion may simply fill its entire cross-section. This is supported by the observation that conversion of T1 acute lesions to chronic black holes is size-dependent (Van Waesberghe et al., 1998).

In conclusion, our results demonstrate different patterns of diffusivity between central and peripheral parts of the MS lesions, and we propose that axonal loss dominates the former, while the effect of de/remyelination may potentially be better detected in the latter. Identifying and separating those patterns has important implications for clinical trials of both neuroprotective and, in particular, remyelinating agents. Disentangling the effects of multiple mechanisms may considerably increase the sensitivity of MRI techniques to monitor subtle changes of axonal loss and myelination.

a) axial view, b) coronal view, c) sagittal view.

Red-T1 hypointense area, Green-"T2-rim" area, Blue-corresponding NAWM area. T1 volume 122 mm^2, T2-rim volume 143 mm^2, contralateral ROI volume-220 mm^2. (For interpretation of the references to color in this figure legend, the reader is referred to the web version of this article.)

References

Alshowaeir, D., Yiannikas, C., Garrick, R., Parratt, J., Barnett, M.H., Graham, S.L., Klistorner, A., 2014. Latency of multifocal visual evoked potentials in nonoptic neuritis eyes of multiple sclerosis patients associated with optic radiation lesions. Invest. Ophthalmol. Vis. Sci. 55, 3758–3764. http://dx.doi.org/10.1167/iovs.14-14571.

Aung, W.Y., Mar, S., Benzinger, T.L., 2014. Diffusion tensor MRI as a biomarker in axonal and myelin damage. Imaging Med. 5, 427–440. http://dx.doi.org/10.2217/iim.13.49. Diffusion.

Bammer, R., Augustin, M., Strasser-Fuchs, S., Seifert, T., Kapeller, P., Stollberger, R., Ebner, F., Hartung, H.P., Fazekas, F., 2000. Magnetic resonance diffusion tensor imaging for characterizing diffuse and focal white matter abnormalities in multiple sclerosis. Magn. Reson. Med. 44, 583–591. http://dx.doi.org/10.1002/1522-2594(200010)44:4<583::AID-MRM12>3.0.CO;2-O.

Barkhof, F., van Walderveen, M., 1999. Characterization of tissue damage in multiple sclerosis by nuclear magnetic resonance. Philos. Trans. R. Soc. Lond. Ser. B Biol. Sci. 354, 1675–1686. http://dx.doi.org/10.1098/rstb.1999.0511.

Barnes, D., Munro, P.M., Youl, B.D., Prineas, J.W., McDonald, W.I., 1991. The longstanding MS lesion. A quantitative MRI and electron microscopic study. Brain 114, 1013–1023.

Brex, P.a., Parker, G.J., Leary, S.M., Molyneux, P.D., Barker, G.J., Davie, C.a., Thompson, a.J., Miller, D.H., 2000. Lesion heterogeneity in multiple sclerosis: a study of the relations between appearances on T1 weighted images, T1 relaxation times, and metabolite concentrations. J. Neurol. Neurosurg. Psychiatry 68, 627–632. http://dx.doi.org/10.1136/jnnp.68.5.627.

Droogan, A.G., Clark, C.A., Werring, D.J., Barker, G.J., McDonald, W.I., Miller, D.H., 1999. Comparison of multiple sclerosis clinical subgroups using navigated spin echo diffusion-weighted imaging. Magn. Reson. Imaging 17, 653–661. http://dx.doi.org/10.1016/S0730-725X(99)00011-9.

Filippi, M., Cercignani, M., Inglese, M., Horsfield, M.A., Comi, G., 2001. Diffusion tensor magnetic resonance imaging in multiple sclerosis. Neurology 56, 304–311.

Filippi, M., Iannucci, G., Cercignani, M., Assunta Rocca, M., Pratesi, A., Comi, G., 2000. A quantitative study of water diffusion in multiple sclerosis lesions and normal-appearing white matter using echo-planar imaging. Arch. Neurol. 57, 1017–1021 (doi:noc90075 [pii]).

Fonov, V.S., Evans, A.C., Botteron, K., Almli, C.R., McKinstry, R.C., L, C.D., BDCG, 2011. Unbiased average age-appropriate atlases for pediatric studies. NeuroImage 54, 313–327.

Janve, V.a., Zu, Z., Yao, S.-Y., Li, K., Zhang, F.L., Wilson, K.J., Ou, X., Does, M.D., Subramaniam, S., Gochberg, D.F., 2013. The radial diffusivity and magnetization transfer pool size ratio are sensitive markers for demyelination in a rat model of type III multiple sclerosis (MS) lesions. NeuroImage 74, 298–305. http://dx.doi.org/10.1016/j.neuroimage.2013.02.034.

Klawiter, E.C., Schmidt, R.B., Trinkaus, K., Liang, H.-F., Budde, M.D., Naismith, R.T., Song, S.-K., Cross, A.H., Benzinger, T.L., 2011. Radial diffusivity predicts demyelination in ex vivo multiple sclerosis spinal cords. NeuroImage 55, 1454–1460.

Klawiter, E.C., Xu, J., Naismith, R.T., Benzinger, T.L., Shimony, J.S., Lancia, S., Snyder, A.Z., Trinkaus, K., Song, S.K., Cross, A.H., 2012. Increased radial diffusivity in spinal cord lesions in neuromyelitis optica compared with multiple sclerosis. Mult. Scler. J. 18, 1259–1268. http://dx.doi.org/10.1177/1352458512436593.

Klistorner, A., Arvind, H., Garrick, R., Yiannikas, C., Paine, M., Graham, S.L., 2010. Remyelination of optic nerve lesions: spatial and temporal factors. Mult. Scler. 16, 786–795. http://dx.doi.org/10.1177/1352458510371408.

Klistorner, A., Sriram, P., Vootakuru, N., Wang, C., Barnett, M.H., Garrick, R., Parratt, J., Levin, N., Raz, N., Van der Walt, A., Masters, L., Graham, S.L., Yiannikas, C., 2014. Axonal loss of retinal neurons in multiple sclerosis associated with optic radiation lesions. Neurology 82, 2165–2172. http://dx.doi.org/10.1212/WNL.0000000000000522.

Klistorner, A., Vootakuru, N., Wang, C., Yiannikas, C., Graham, S.L., Parratt, J., Garrick, R., Levin, N., Masters, L., Lagopoulos, J., Barnett, M.H., 2015. Decoding diffusivity in multiple sclerosis: analysis of optic radiation lesional and non-lesional white matter. PLoS One 10, e0122114. http://dx.doi.org/10.1371/journal.pone.0122114.

Kolasinski, J., Stagg, C.J., Chance, S.a., Deluca, G.C., Esiri, M.M., Chang, E.-H., Palace, J.a., McNab, J.a., Jenkinson, M., Miller, K.L., Johansen-Berg, H., 2012. A combined post-mortem magnetic resonance imaging and quantitative histological study of multiple sclerosis pathology. Brain 135, 2938–2951. http://dx.doi.org/10.1093/brain/aws242.

Lassmann, H., Suchanek, G., Ozawa, K., 1994. Histopathology and the blood-cerebrospinal fluid barrier in multiple sclerosis. Ann. Neurol. 36 (Suppl), S42–S46.

Loevner, L.A., Grossman, R.I., McGowan, J.C., Ramer, K.N., Cohen, J.A., 1995. Characterization of multiple-sclerosis plaques with T1-weighted Mr and quantitative magnetization-transfer. Am. J. Neuroradiol. 16, 1473–1479.

Mädler, B., Drabycz, S.a., Kolind, S.H., Whittall, K.P., MacKay, A.L., 2008. Is diffusion anisotropy an accurate monitor of myelination? Correlation of multicomponent T2 relaxation and diffusion tensor anisotropy in human brain. Magn. Reson. Imaging 26, 874–888. http://dx.doi.org/10.1016/j.mri.2008.01.047.

Miller, D.H., 2008. Neuroimaging in multiple sclerosis. In: Raine, C.S., Mcfarland, H.F., Hohlfeld, R. (Eds.), Multiple Sclerosis. Elsevier, Edinburgh, pp. 69–87.

Mohammadi, S., Carey, D., Dick, F., Diedrichsen, J., Sereno, M.I., Reisert, M., Callaghan, M.F., Weiskopf, N., 2015. Whole-brain in-vivo measurements of the axonal G-ratio in a group of 37 healthy volunteers. Front. Neurosci. 9, 1–13. http://dx.doi.org/10.3389/fnins.2015.00441.

Nijeholt, G.J., Bergers, E., Kamphorst, W., Bot, J., Nicolay, K., Castelijns, J.a., van Waesberghe, J.H., Ravid, R., Polman, C.H., Barkhof, F., 2001. Post-mortem high-resolution MRI of the spinal cord in multiple sclerosis: a correlative study with conventional

MRI, histopathology and clinical phenotype. Brain 124, 154–166. http://dx.doi.org/10.1093/brain/124.1.154.

Nusbaum, A.O., Lu, D., Tang, C.Y., Atlas, S.W., 2000. Quantitative diffusion measurements in focal multiple sclerosis lesions: correlations with appearance on T1-weighted images. Am. J. Roentgenol. 175, 821–825. http://dx.doi.org/10.2214/ajr.175.3.1750821.

Polman, C.H., Reingold, S.C., Banwell, B., Clanet, M., Cohen, J.a., Filippi, M., Fujihara, K., Havrdova, E., Hutchinson, M., Kappos, L., Lublin, F.D., Montalban, X., O'Connor, P., Sandberg-Wollheim, M., Thompson, A.J., Waubant, E., Weinshenker, B., Wolinsky, J.S., 2011. Diagnostic criteria for multiple sclerosis: 2010 revisions to the McDonald criteria. Ann. Neurol. 69, 292–302. http://dx.doi.org/10.1002/ana.22366.

Rovaris, M., Gass, A., Bammer, R., Hickman, S.J., Ciccarelli, O., Miller, D.H., Filippi, M., 2005. Diffusion MRI in multiple sclerosis. Neurology 65, 1526–1532.

Sbardella, E., Tona, F., Petsas, N., Pantano, P., 2013. DTI measurements in multiple sclerosis: evaluation of brain damage and clinical implications. Mult. Scler. Int. 2013, 671730. http://dx.doi.org/10.1155/2013/671730.

Scanderbeg, A.C., Tomaiuolo, F., Sabatini, U., Nocentini, U., Grasso, M.G., Caltagirone, C., 2000. Demyelinating plaques in relapsing-remitting and secondary-progressive multiple sclerosis: assessment with diffusion MR imaging. Am. J. Neuroradiol. 21, 862–868.

Schmierer, K., Parkes, H.G., So, P.-W., 2009. Direct visualization of remyelination in multiple sclerosis using T2 weighted high-field MRI. Neurology 72, 2008–2009. http://dx.doi.org/10.1212/01.wnl.0000341878.80395.39.Direct.

Schmierer, K., Wheeler-Kingshott, C.a.M., Tozer, D.J., Boulby, P.a., Parkes, H.G., Yousry, T.a., Scaravilli, F., Barker, G.J., Tofts, P.S., Miller, D.H., 2008. Quantitative magnetic resonance of postmortem multiple sclerosis brain before and after fixation. Magn. Reson. Med. 59, 268–277. http://dx.doi.org/10.1002/mrm.21487.

Schmierer, K., Wheeler-Kingshott, C.A.M., Boulby, P.A., Scaravilli, F., Altmann, D.R., Barker, G.J., Tofts, P.S., Miller, D.H., 2007. Diffusion tensor imaging of post mortem multiple sclerosis brain. NeuroImage 35, 467–477. http://dx.doi.org/10.1016/j.neuroimage.2006.12.010.

Song, S.-K., Yoshino, J., Le, T.Q., Lin, S.-J., Sun, S.-W., Cross, A.H., Armstrong, R.C., 2005. Demyelination increases radial diffusivity in corpus callosum of mouse brain. NeuroImage 26, 132–140. http://dx.doi.org/10.1016/j.neuroimage.2005.01.028.

Van Waesberghe, J.H.T.M., Van Walderveen, M.A.A., Castelijns, J.A., Scheltens, P., Lycklama a Nijeholt, J.G., Polman, C.H., Barkhof, F., 1998. Patterns of lesion development in multiple sclerosis: longitudinal observations with T1-weighted spin-echo and magnetization transfer MR. Am. J. Neuroradiol. 19, 675–683.

van Walderveen, A.A.A., Kamphorst, W., Scheltens, P., van Waesberghe, J.H.T.M., Ravid, R., Valk, J., Polman, C.H., Barkhof, F., 1998. Histopathologic correlate of hypointense lesions on Tl-weighted spin-echolesions on Tl-weighted spin-echo MRI in multiple sclerosis MRI in multiple sclerosis. Neurology 50, 1282–1288.

Wang, Y., Sun, P., Wang, Q., Trinkaus, K., Schmidt, R.E., Naismith, R.T., Cross, A.H., Song, S.-K., 2015. Differentiation and quantification of inflammation, demyelination and axon injury or loss in multiple sclerosis. Brain 138, 1223–1238. http://dx.doi.org/10.1093/brain/awv046.

Wang, Y., Wang, Q., Haldar, J.P., Yeh, F.C., Xie, M., Sun, P., Tu, T.W., Trinkaus, K., Klein, R.S., Cross, A.H., Song, S.K., 2011. Quantification of increased cellularity during inflammatory demyelination. Brain 134, 3587–3598. http://dx.doi.org/10.1093/brain/awr307.

Werring, D.J., Clark, C.A., Barker, G.J., Thompson, A.J., Miller, D.H., 1999. Diffusion tensor imaging of lesions and normal-appearing white matter in multiple sclerosis. Neurology 52, 1626. http://dx.doi.org/10.1212/WNL.52.8.1626.

Wheeler-Kingshott, C.A.M., Cercignani, M., 2009. About "axial" and "radial" diffusivities. Magn. Reson. Med. 61, 1255–1260.

Winston, G.P., 2012. The physical and biological basis of quantitative parameters derived from diffusion MRI. Quant. Imaging Med. Surg. 2, 254–265. http://dx.doi.org/10.3978/j.issn.2223-4292.2012.12.05.

Yeatman, J.D., Dougherty, R.F., Myall, N.J., Wandell, B.a., Feldman, H.M., 2012. Tract profiles of white matter properties: automating fiber-tract quantification. PLoS One 7, e49790. http://dx.doi.org/10.1371/journal.pone.0049790.